

RD50 overview: development of radiation hard detectors for high luminosity colliders

Marcos Fernández García^{*†}

Instituto de Física de Cantabria (IFCA), CSIC-Universidad de Cantabria, Ed. Juan Jordá,

Avda. los Castros s/n, Santander E-39005, Spain

E-mail: Marcos.Fernandez@cern.ch

RD50 (Radiation Hard Semiconductor Devices For High Luminosity Colliders) is a transversal CERN R&D collaboration across different experiments interested in pushing the radiation hardness of current silicon detectors. Activity in the collaboration is organized in 4 fronts: defect and material characterization (mapping microscopic features to macroscopic properties of devices), detector characterization (including development of new measurement techniques, like edge-TCT or Two Photon Absorption TCT), new structures (3D sensors, detectors with amplification, slim edges, ...) and finally full detector systems (studying the operation of detectors up to LHC readout frequencies and rates). A device simulation subgroup is in charge of understanding the performance of actual devices and projecting the endurance of these devices in the long term.

The 23rd International Workshop on Vertex Detectors,

15-19 September 2014

Macha Lake, The Czech Republic

^{*}Speaker.

[†]On behalf of the RD50 collaboration

1. Introduction

RD50 is a CERN R&D collaboration [1] in charge of finding ways to develop radiation hard semiconductor devices for high luminosity colliders. It comprises at this moment 275 members from 50 institutes and 42 countries. It was created in 2001, after the successful completion of the CERN RD48 (also known as ROSE) collaboration [2] which engineered a silicon detector able to survive the first 10 years of operation of the LHC. RD48 found that, by diffusing oxygen into silicon, the radiation tolerance – expressed as increase of depletion voltage with fluence – was better than for standard silicon, but only if irradiated with charged hadrons. Diffusion Oxygenated Float Zone (DOFZ) Silicon was then chosen as material for the vertex detectors, placed in an environment dominated by charged hadron flux. No beneficial effect was found for neutron irradiated devices. However, measurements of n-type silicon diodes of different resistivities also showed that low resistivity material ($\approx 1k\Omega\text{-cm}$), despite requiring a higher initial depletion voltage, displayed delayed type inversion and lead to lower depletion voltage under neutron irradiation. This low resistivity material was then proposed as the best option for silicon microstrips populating outer regions, where the flux is dominated by neutrons coming from the breakup of nuclei after hadronic impacts in the calorimeter.

The ultimate goal of RD50 is to develop radiation hard devices that will cope with a maximal fluence of $2 \times 10^{16} \text{ n}_{\text{eq}}/\text{cm}^2$, as expected after 10 years of LHC running at high luminosity (HL-LHC). While material engineering yielded a solution to the hardening of silicon in the LHC, the factor 10 increase in fluence requires this time a combined material and device engineering approach. Some of the technology considered within RD50 and summarized in this document comprises the following:

- Choice of electron collection (n^+ readout) in p-bulk material.
- Thin detectors (thinner than standard $300 \mu\text{m}$ bulk).
- New sensor schemes like, for instance, 3D or HV-CMOS sensors. In the first case, 3D sensors, the depletion volume is decoupled from the active collection volume by setting columnar electrodes in the bulk. HV-CMOS, on the other hand, are depleted Monolithic Active Pixels benefiting from industrialized CMOS processes where charge is collected by drift in a low resistivity bulk.

Other approaches, like modifications to the standard sensor design, are pursued as well. Some of them include: reduction of inactive area for detection (slim edge detectors), extension of active area to the very edge of the detector (active edges), exploitation of charge multiplication induced by irradiation (detector with implant trenches or geometrically optimized to enhance multiplication) or built-in already before irradiation (Low Gain Avalanche Detectors).

2. Material engineering: from microscopical defects to macroscopic properties

Although the beneficial effect of Oxygen in the radiation hardness of silicon was discovered by the ROSE collaboration, the microscopical reason was not unveiled until recently [3]. Fig-

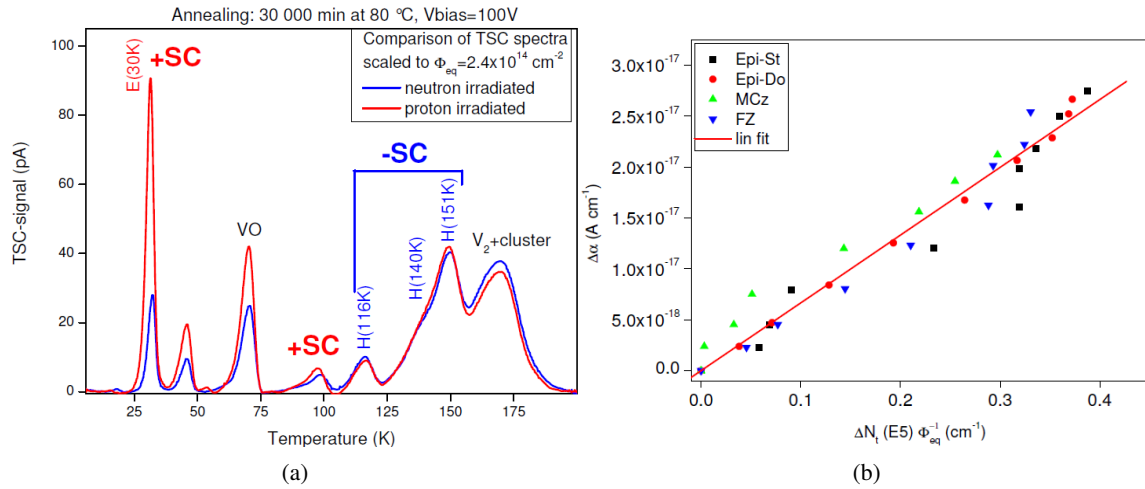


Figure 1: a) TSC measurements for 1 MeV neutron (blue) and 23 GeV proton (red) of an oxygen rich silicon sample, showing compensation of positive space charge of donor E30K compared to the negative charge of the acceptor H-defects. Research from [3], reprinted after [4]. b) Correlation of the E5 defect concentration with the change in the damage parameter for Epi-Standard, Epi-DO, MCZ and FZ material [4].

Figure 1.a) shows the TSC (Thermally Stimulated Current) signal¹ for an n-bulk oxygen-rich epitaxial diode irradiated with protons or neutrons. While both types of radiation introduce deep acceptors (negative space charge, defects H(116K,140K,151K)), the proton irradiation produces a surplus of donors (positive space charge, defect E(30K)) in oxygenated materials. This excess of positive space charge avoids space charge type inversion (SCSI) from positive to negative. In turn, the three cluster-related defects H(116K,140K,151K), revealed as deep hole traps, proved to be responsible specifically for the reverse annealing [6].

Defects responsible for the increase of leakage current after neutron and charged hadron irradiation were identified in 2007 [7]. Defects close to the middle of the bandgap are known to act as recombination-generation centers and are efficiently producing leakage current. The leakage current is also known to anneal with time. This annealing is a result of the dissolution of defects in the silicon crystal [4]. By comparing DLTS (Deep Level Transient Spectroscopy) spectra measured during the annealing of FZ diodes, it was possible to correlate the decrease of the DLTS signal with the decrease of leakage current. Two cluster defects were tagged to produce the current: the trivacancy E5 and the E205a defect. Figure 1.b) shows the correlation of the E5 defect concentration with the change of damage parameter α for the leakage current.

3. Simulation

Due to computational limitations, the implementation of the complete set of identified defects into TCAD (Technology Computer Aided Design) simulations [8], aiming to reproduce the effect of radiation in realistic devices, is not feasible. Therefore, models are used where few effective

¹Experimental method where a sample is cooled to very low temperatures, then flooded with carriers and heated up such that the trapped charges give raise to current peak signals. See section 4.5 in [5] for details.

defects are considered. These effective defect levels do not necessarily coincide with any of the measured ones. For the moment, there is no universal set of parameters that describes all the measurements of different sensors and irradiation stages. Defect parameters have been worked out to account for leakage current increase with fluence, space charge sign inversion (SCSI), double junction effect in TCT (Transient Current Technique) measurements and trapping in Charge Collection Efficiency measurements for specific set of measurements. Within the RD50 collaboration, the starting point is a 2 defect model proposed in [9]. For example, this model has been used and refined for the CMS Phase 2 upgrade campaign (CMS HPK campaign), as described in [10].

All the above mentioned macroscopic parameters are related to bulk damage. However proton irradiation, for instance, is known to produce not only bulk but also surface damage. Surface damage has been usually neglected in our community, because it does not impact directly on operational parameters like the leakage current or depletion voltage. Recent works within the RD50 and CMS simulation workgroups [11, 12] have implemented surface damage considering both oxide charge density and interface traps by including 2 extra defects at the interface of silicon with its native oxide. As a result, effects like extra noise hits of p-on-n detectors or interstrip resistance measurements have been explained [13].

4. RD50 recommendations on material choice towards HL-LHC

Recommendations on bulk type:

RD50 has proposed the usage of electron readout as a radiation hard technology for the HL-LHC [14]. P-bulk detectors (n-on-p, also referred to as n-type readout) collect both electrons (at the segmented side) and holes (at the backelectrode). However, due to the asymmetry of the weighting field, the charge induced by the carriers moving to the segmented side is higher than the one induced by carriers drifting to the unstructured side. On top of that, collection of electrons is more efficient than the collection of holes. There are several arguments that support this statement.

Charge collection: both the weighting field and the electric field of the detector are maxima at the segmented side of p-bulk detectors. For n-bulk devices, instead, the electric field will move to the backplane (SCSI) after few 10^{14} n_{eq}/cm^2 , and the scalar product of electric and weighting fields (determining the mathematical magnitude of the induced current) will diminish. Another reason for electron collection comes from the higher mobility of electrons over holes: for equal field intensity, electrons will be collected faster than holes.

Trapping: due to the faster mobility of electrons, trapping can be less harmful for n-type readout, overall in thin bulk detectors. On top of that, annealing of trapping is beneficial for electrons while it increases for holes, as it has been experimentally measured [15].

Charge multiplication: electrons need less field intensity than holes to produce secondary ionizations, so they can multiply close to the electrodes, provided the field is high enough there.

Long term annealing of the signal: while n-bulk detectors show annealing of the depletion voltage and collected signal, p-bulk sensors only showed depletion voltage annealing with time. Here slightly different trends have been identified by ATLAS and CMS throughout their

upgrade campaigns targeted towards HL-LHC. While ATLAS found no annealing of the collected signal [16]), CMS, on the other hand, found that up to 1.5×10^{15} n_{eq}/cm^2 (strip region), only thick (300 μm) sensors have signal annealing [17]. Thinner detectors did not exhibit signal annealing. Absence of annealing in the collected charge will ease operation of the tracker, since beneficial annealing of the leakage current at room temperature can be exploited without a decrease of the collected charge.

Recommendations on sensor thickness:

The choice of thickness for the sensors is driven by many factors: contribution to multiple scattering, power consumption (via leakage current), annealing behavior (see paragraph above), charge multiplication (favored in thinner sensors due to higher E-field at the same bias voltage), depletion voltage after irradiation, detector geometry (see for instance the interplay of geometry with sensor thickness in [18]), trapping, price of the thinning process...

Studies of charge collection of n-on-p planar pixel devices [19] of different thickness from various manufacturers (MPI HLL [20] and CiS [21]), and readout with FEI3 [22] and FEI4 [23], show that at moderate voltages (200-300V) and fluences below 5×10^{15} n_{eq}/cm^2 optimum thickness is about 150 μm . For fluences one order of magnitude above, signal from thin and thick detectors equalizes, so the extra signal obtained from a thicker bulk is compensated by higher trapping. From a signal-only point of view, ~ 150 μm seems to be the optimum thickness for HL-LHC pixels.

For strips region ($\Phi_{eq} \leq 1.5 \times 10^{15}$ n_{eq}/cm^2) the CMS HPK campaign has made a thorough comparison of 300 and 200 μm thick FZ and MCZ detectors (see for instance [17]). As irradiated and after short term annealing, thick FZ detectors collect more (seed) signal up to 10^{15} n_{eq}/cm^2 (see Fig. 2.a)). During annealing, thick detectors give more collected charge up to 20 weeks at RT ($\approx 8h$ at $60^\circ C$). After this time (Fig. 2.b)), charge collection for 200 μm thick n-on-p MCZ detectors is higher than for 300 μm thick for voltages up to 700V. Above this value, thick FZ n-on-p detectors will collect more charge.

5. New devices

Complementary to material engineering, device engineering offers new solutions to reach radiation hardness in excess of 10^{16} n_{eq}/cm^2 . Optimization of existing devices or completely new sensor paradigms can provide enhanced resistance to radiation. Examples of optimized sensors could be microstrips tuned to enhance charge multiplication after irradiation [24]. New devices heavily developed in the RD50 collaboration are, among others:

- 3D devices, with columnar implants across the bulk, where depletion grows sideways, instead of vertically. Smaller interdistance between the n^+ and p^+ implants (compared to planar detectors) allows a reduction of the depletion voltage for the same detector thickness. More information about 3D devices can be found in this conference [25]. These detectors already populate 25% of the installed Insertable B-layer pixel system of the ATLAS experiment.
- Low Gain Avalanche Diodes (LGADs) utilize a deep p-well below the n-implantation on a high resistivity p-type substrate. The sharp space charge change at the interface of the 2 implanted regions leads to an increased electric field intensity above the impact ionization

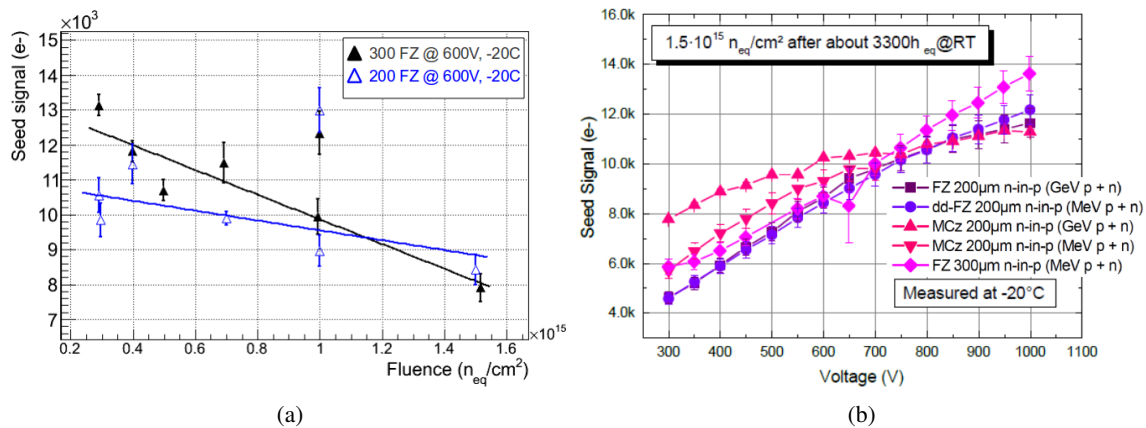


Figure 2: a) Charge collected on the seed strip (strip with highest signal in a cluster) vs. fluence (600V, -20C, short annealed samples (less than 250h at room temperature)) for 320 and 200 μm thickness. Lines drawn to guide the eye. b) Charge collection vs. bias voltage after $1 \times 10^{15} n_{eq}/\text{cm}^2$ and 3300 h annealing at room temperature. Plots taken from [17].

limit of electrons. Therefore drifting electrons can produce additional e-h pairs. This phenomenon is called charge multiplication. The technological parameter that controls the gain factor is the implantation dose of the deep p-well. Both pixels and strips are targets for this technology. Multiplication needs to be "low" because the detector has to be able to use the same readout electronics as their non-multiplying counterparts. This avoids redesigning new readout electronics. Low gain is also needed for high voltage stability of irradiated detectors, where high fields can build up near the electrodes, where multiplication occurs. Radiation damage of these devices is under study [26, 27]. A review of this technology can also be found in this conference [28].

- CMOS pixels in HV technology, built on low resistivity p-type silicon. Using a wide and deep n-well, charge is collected by drift (due to a small depleted volume of the low resistivity substrate) and partly by diffusion (at least for non irradiated devices). To confirm this, laser TCT measurements under edge illumination configuration (edge-TCT) have been carried out. Details are given in the next section.

Finally, other developments within RD50 pursue modifications to detectors aimed to improve their sensing performance as sensors, without making an impact on their radiation hardness. This category includes modifications of the edges of the detectors, such that less inactive region lies between the active volume and the cutting edge of the detector. The technologies that allow this are slim edge detectors and active edge detectors. More information about them can be found as well in this conference [29].

In the next section we report on one of these technologies where the author has made a contribution.

Pixels with built-in gain: HV-CMOS

Pixel detectors in standard CMOS technologies have gained popularity in recent years. The

STAR tracker (MIMOSA MAPs [30]), Belle-II (with DEPFET [31]) and ALICE ITS upgrade [32] are examples of experiments using monolithic CMOS pixels for the inner pixel layers. These technologies are also considered as valid options for ILC and CLIC.

CMOS monolithic active pixels (MAPs) offer a low-cost solution for the construction of silicon trackers because they utilize commercially available technologies providing, for instance, in-pixel amplification and discrimination or wafer thinning. They achieve smaller pixel sizes than hybrid systems and do not need bump bonding to a readout chip, reducing the mechanical complexity. Charge transport happens by diffusion in a thin undepleted 5-25 μm epi-layer (substrate). Charges may eventually reach a small (but depleted) n-well/p-epi junction where they get finally collected. Since most of the charge transport is by diffusion (typical times >100 ns), MAPs are slow and for that reason, more affected by trapping than detectors collecting signal by drift only. Another limitation of MAPs in their original form is that only NMOS transistors (housed on p-wells) can be built inside the p-bulk substrate. A PMOS transistor in an n-well would compete in charge collection with the collecting n-well.

In a new detector concept, the High Voltage monolithic detector built on HV-CMOS technology, the small n-well collecting diode is replaced by a long and deep n-well. Inside this n-well, NMOS and PMOS transistors can be used (which means that any complex electronics might in principle be built inside). The PMOS transistors are actually placed in a shallow n-well inside the deep n-well, ohmically connected to it. The shallow n-well is biased using a high resistance or reset switch [33]. The extended deep n-well allows partial depletion of the highly doped region lying underneath. Charge produced in the depleted region will drift, and collection will happen within few nanoseconds. Extra charge may also appear in the depleted region after diffusion from the undepleted bulk (unirradiated detector) or after drift from the neutral bulk (highly irradiated detector [9]). Since charge is collected by drift, it is expected that these detectors will be more radiation hard than the diffusion-only MAPs counterparts.

Depending on the used HV technology, the extended junction can be biased up to ≈ 100 V. For a conservative bias voltage of 60 V and a bulk of $10 \Omega \cdot \text{cm}$, the depletion width is $\approx 10 \mu\text{m}$. To quantify this statement, edge-TCT measurements of irradiated samples have been performed in the third version of the chip (HVC MOSv3). The chip implements both a matrix of pixels on a deep n-well, and an isolated deep n implant forming an n-p diode ($100 \times 100 \mu\text{m}^2$) close to the edge of the detector. The latter was included in the design to ease edge-TCT measurements and provides direct access to the analog output (no CMOS active electronics involved).

In edge-TCT [34], a strongly focused ($\sigma \approx 8 \mu\text{m}$) laser beam is pointed at the edge of a detector and is scanned across its thickness². The penetration depth of the photons inside the bulk depends on the wavelength. For instance, near-infrared light (1060 nm, 1 mm absorption length) reaches features well beyond the cutting edge (and guard rings) of the detector. In a standard edge-TCT measurement, the beam is scanned vertically along the edge of the sensor, from top to bottom, and the instantaneous induced currents are studied as a function of depth and bias voltage. The signal from the detector is amplified using a fast current amplifier [35] and directly read out using an oscilloscope (2.5 GHz). By integrating the current waveforms we can map regions of the detector

²In edge-TCT light incidence is orthogonal to standard top/bottom TCT where light is pointed perpendicular to the surface.

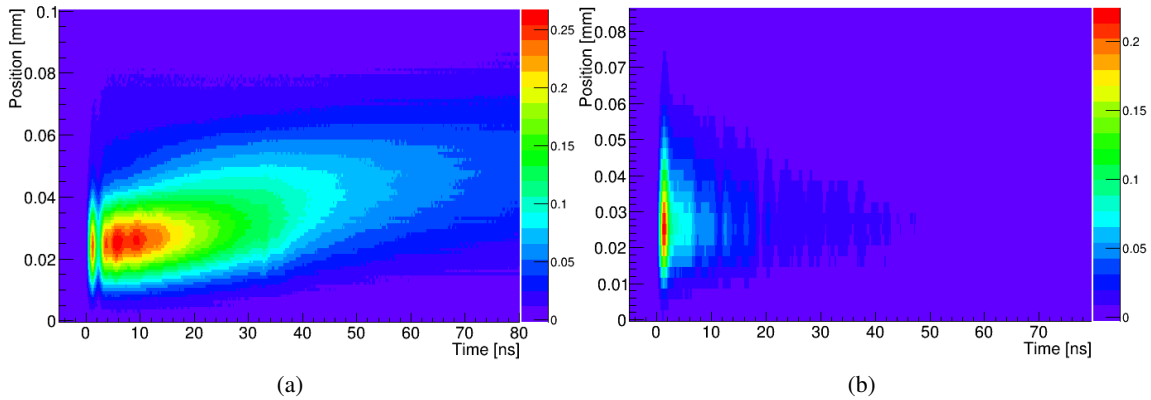


Figure 3: a) Signal map displaying in a color scale, the time resolved induced signal in the detector as a function of the depth (arbitrary choice of ordinates origin). The top face of the detector is located approximately at $z = 0$, the z axis pointing into the wafer. The detector is scanned in the center of the isolated test diode, using full chip readout. b) Same as in a) but for the detector irradiated to $2 \times 10^{16} \text{ n}_{\text{eq}}/\text{cm}^2$ [36].

efficient for charge collection.

Three neutron irradiated [37] $(1.5, 7, 20) \times 10^{15} \text{ n}_{\text{eq}}/\text{cm}^2$ and one non-irradiated HVCMOSv3 detectors were measured in edge-TCT at CERN [38]. The detectors were mounted on a custom designed PCB [39] which allowed for different readout schemes. For instance, in the so-called "full-chip readout" configuration, all the components of the detector are grounded while the high voltage is applied to the ohmic contact of the bulk. The signal produced anywhere in the detector is studied in this configuration. In the "diode readout configuration", only the isolated diode is connected to the amplifier while the rest of the detector remains grounded. In this configuration only the signal induced immediately below or around the diode is collected.

Fig. 3 shows a 2D plot of the time resolved induced current (coded in colors) as a function of transient time and depth in the bulk. The detector was biased at 40V, which should be enough to deplete approximately $10 \mu\text{m}$ below the deep N-well. The diode was scanned vertically along its center, entering the detector from top ($z=0$), then going deeper in the bulk ($z>0$). Two distinctive timewise contributions are observed: a fast signal that lasts $\approx 2 \text{ ns}$ and extends for $\approx 40 \mu\text{m}$ inside the bulk, and a much slower component (time scale $>100 \text{ ns}$) over $\approx 80 \mu\text{m}$ in the bulk (due to the convolution with the width of the laser spot, the raw image gives an overestimation of the active volume). The fast contribution is interpreted as drift of carriers produced directly inside the depleted region by the laser (gaussian width $8 \mu\text{m}$). The slow one is associated to charge carriers diffusing in the undepleted volume and eventually entering the depleted region. The same scan, repeated for a detector irradiated to the maximum fluence $2 \times 10^{16} \text{ n}_{\text{eq}}/\text{cm}^2$ and biased at 80 V, shows still a fast contribution and a much smaller slow contribution. At $2 \times 10^{16} \text{ n}_{\text{eq}}/\text{cm}^2$, the trapping time for electrons is 125 ps and the drift length is only $12.5 \mu\text{m}$ [40]. Therefore it seems unlikely that a slow diffusion process may contribute to the signal formation in highly irradiated detectors. At this moment, a clear interpretation of this data based on TCAD simulations is missing. In highly irradiated detectors, a double junction has been reported, consisting of space

charge of opposite sign near the electrodes separated by a central neutral, almost-intrinsic, region where a small uniform electric field is present. This field leads to an injection of slow carriers back to the main depleted regions. This could be an explanation for the observed slow signal in the $2 \times 10^{16} \text{ n}_{\text{eq}}/\text{cm}^2$ sample.

Finally, Fig. 4 shows the comparison of the depleted region at 60V for the detector irradiated to $2 \times 10^{16} \text{ n}_{\text{eq}}/\text{cm}^2$ and the unirradiated detector at the same voltage. The plot shows the collected charge as a function of the depth of the beam inside the detector. The scans of the detector were taken at the same laser power. Two things are clear from this comparison. The first is that the depleted width is very similar for both fluences, the second that the collected charge for the irradiated detector is 40% of that of the unirradiated detector, pointing at the removal of charge carriers by trapping.

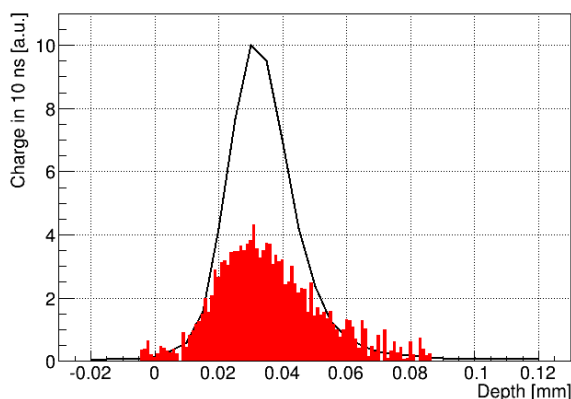


Figure 4: Collected charge at 60V for an unirradiated detector (simple line) compared to the detector irradiated to highest fluence ($2 \times 10^{16} \text{ n}_{\text{eq}}/\text{cm}^2$). The depleted width is very similar in both cases. The difference in maximum amplitude is related to trapping [36].

6. Summary and outlook

RD50 is a CERN R&D collaboration integrated by members from 42 countries and different experiments, striving to extend radiation hardness of current silicon detectors beyond current limits. The problem is approached from different directions, from material engineering (intentional doping of the bulk to improve radiation properties) to device engineering (tuning of existing designs, brand new detector schemes). Along this path comes the development of new characterization techniques, like edge-TCT or Two Photon Absorption-TCT [41], both developed in the framework of radiation hardness studies within RD50.

RD50 has been instrumental for the choice of bulk material for HL-LHC experiments. The potential of electron readout was early identified. Effects like charge multiplication in irradiated devices were first spotted, then exploited as a means to reduce material budget without any detriment of the signal. Effects like the double peak structure of induced currents in irradiated detectors were explained and concepts like depletion voltage and effective doping concentration were redefined.

Studies of silicon at fluences of 10^{17} n_{eq}/cm² [42] have already been reported in the collaboration. This is already one order of magnitude higher than needed for the Phase 2 upgraded LHC. The good news for the community is that silicon is still alive at these fluences.

References

- [1] CERN R&D Proposal, LHCC 2002-003/P6, 15.2.2002, <http://www.cern.ch/rd50>.
- [2] Research and development On Silicon for future Experiments The RD48 collaboration: <http://rd48.web.cern.ch/RD48>.
- [3] I. Pintilie et al., *Radiation-induced point- and cluster-related defects with strong impact on damage properties of silicon detectors*, Nucl. Instr. Meth. A 611 (2009) 52-68, doi:10.1016/j.nima.2009.09.065.
- [4] A. Junkes, *Influence of radiation induced defect clusters on silicon particle detectors*, Ph.D. thesis, DESY-THESIS-2011-031, July 2011.
- [5] M. Moll, *Radiation Damage in Silicon Particle Detectors – Microscopic Defects and Macroscopic Properties –*, Ph.D. thesis, DESY-THESIS-1999-040, December 1999.
- [6] I. Pintilie et al., *Appl. Phys. Letters* 92, 024101 (2008).
- [7] R.M. Fleming, *Appl. Phys. Letters* 90, 172105 (2007), doi:10.1063/1.2731516.
- [8] Synopsys, Inc., Synopsys TCAD services, 2009, <http://www.synopsys.com/Tools/TCAD>.
- [9] V. Eremin et al., *The origin of double peak electric field distribution in heavily irradiated silicon detectors*, Nucl. Instr. Meth. A, 476 (2002) 556.
- [10] R. Eber, *Untersuchung neuartiger Sensorkonzepte und Entwicklung eines effektiven Modells der Strahlenschädigung für die Simulation hochbestrahlter Silizium-Teilchendetektoren*. Phd. thesis, IEKP-KA/2013-27.
- [11] T. Peltola, *Silicon Sensors for Trackers at High-Luminosity Environment – RD50*, RESMDD14 conference, 8-10 October 2014, Firenze, Italy.
- [12] R. Dalal, *Simulation of irradiated detectors*, Proceedings of this conference.
- [13] R. Dalal et al., *Combined effect of bulk and surface damage on strip insulation properties of proton irradiated n⁺-p silicon strip sensors*, 2014 JINST 9 P04007.
- [14] G Casse et al., *Improving the radiation hardness properties of silicon detectors using oxygenated n-type and p-type silicon*, IEEE Trans. Nucl. Sci., Vol. 47, No. 3, June 2000.
- [15] O. Krasel, *Charge Collection in Irradiated Silicon-Detectors*, Ph.D. thesis, Un. Dortmund, 2004.
- [16] G. Casse et al., *Effects of accelerated annealing on p-type silicon micro-strip detectors after very high doses of proton*, Nucl. Instr. Meth. A 568 (2006) 46-50.
- [17] A. Dierlamm et al., draft version of *Technical Proposal for the phase-2 upgrade of the Compact Muon Solenoid*, to be published.
- [18] G. Kramberger, D. Contarato, Nucl. Instr. Meth. A, 560 (2006) 98-102.
- [19] S.Terzo. *Irradiated n-in-p planar pixel sensors with different thicknesses and active edge designs*, 23rd RD50 Workshop, November 2013.
- [20] Halbleiterlabor der Max-Planck-Gesellschaft, Otto-Hahn-Ring 6, D-81739 München.

- [21] CiS Forschungsinstitut für Mikrosensorik und Photovoltaik GmbH, Konrad-Zuse-Strasse 14, 99099 Erfurt, Germany.
- [22] I. Peric et al., The FEI3 readout chip for the ATLAS pixel detector, Nucl. Instrum. Meth. A565 (2006) 178.
- [23] M. Garcia-Sciveres et al., *The FE-I4 pixel readout integrated circuit*, Nucl. Instr. Meth. Volume 636, Issue 1, Supplement, 21 April 2011, Pages S155-S159.
- [24] C. Betancourt et al., *A charge collection study with dedicated RD50 charge multiplication sensors*, Nucl. Instr. Meth. A 730 (2013)62-65.
- [25] S. Grinstein, *3D detectors in ATLAS*, Proceedings of this conference.
- [26] G. Kramberger, *Studies of CNM diodes with gain*, 22nd RD50 Workshop, 3-6 June 2013, Albuquerque, USA.
- [27] G. Kramberger, *Studies of LGAD diodes in Ljubljana (an update)*, 23rd RD50 Workshop (CERN), 13-15 November 2013.
- [28] V. Greco, *Devices optimised for avalanche multiplication*, Proceedings of this conference.
- [29] A. J. Blue, *Edgeless and slim-edge detectors*, Proceedings of this conference.
- [30] R. Turchetta et al., *A monolithic active pixel sensor for charged particle tracking and imaging using standard VLSI CMOS technology*, Nucl. Instr. Meth. Vol. 458, Issue 3, 11 February 2001, pp. 677-689.
- [31] J. Kemmer, G. Lutz, *New detector concepts*, Nucl. Instr. Meth. 253, 3, 1987, S. 365-377.
- [32] ALICE Collaboration, *Technical Design Report for the Upgrade of the ALICE Inner Tracking System*, CERN-LHCC-2013-024 ; ALICE-TDR-017
- [33] I. Peric, *Habilitation thesis*, Ruprecht - Karls - University Heidelberg, April 2010.
- [34] G. Kramberger, IEEE Transactions on Nuclear Science, Vol. 57, No. 4, August 2010.
- [35] Cividec 2, 2 GHz current amplifier, <http://www.cividec.at/>.
- [36] M.F. García, *Edge-TCT characterization of irradiated HV-CMOSv3 sensors*, to be published.
- [37] Reactor TRIGA, Jozef Stefan Institute, Jamova 39, 1000 Ljubljana, Slovenia
<http://www.rcp.ijs.si/ric/index-a.htm>.
- [38] Solid State Detectors Support and R&D, PH-DT group, CERN.
<http://ssd-rd.web.cern.ch/ssd-rd/>.
- [39] PCB design by Constantin Weisser, CERN Summer Student program 2014.
<http://cds.cern.ch/record/1755270?ln=en>.
- [40] G. Kramberger et al., *Annealing studies of effective trapping times in silicon detectors*, Nucl. Instr. Meth. A 571 (2007) 608-611.
- [41] R. Palomo, *Two Photon Absorption and carrier generation in semiconductors*, 25th RD50 workshop, CERN, November 2014.
- [42] M. Mikuz, *Electric field and mobility in extremely irradiated silicon*, 25th RD50 workshop, CERN, November 2014.